

Original Paper

Peptidylarginine Deiminases Inhibitors Decrease Endothelial Cells Angiogenic Potential by Affecting Akt Signaling and the Expression and Secretion of Angiogenic Factors

Oskar Ciesielski^{a,b} Luciano Pirola^c Aneta Balcerczyk^a

^aDepartment of Oncobiology and Epigenetics, Faculty of Biology and Environmental Protection, University of Lodz, Pomorska 141/143, Lodz 90-236, Poland, ^bThe Bio-Med-Chem Doctoral School of the University of Lodz and Lodz Institutes of the Polish Academy of Sciences, University of Lodz, Banacha 12/16, 90-237 Lodz, Poland, ^cCarMeN Laboratory, INSERM Unit 1060, Lyon-1 University, 165 Chemin du Grand Revoyet, BP12, 69495, Pierre Bénite Cedex, France

Key Words

Citrullination • PADs inhibitors • Endothelial cells • Angiogenesis • Akt signaling

Abstract

Background/Aims: Endothelial cells (ECs) play a crucial role in various physiological processes, particularly those related to the cardiovascular system, but also those affecting the entire organism. The biology of ECs is regulated by multiple biochemical stimuli and epigenetic drivers that govern gene expression. We investigated the angiogenic potential of ECs from a protein citrullination perspective, regulated by peptidyl-arginine deiminases (PADs) that modify histone and non-histone proteins. Although the involvement of PADs has been demonstrated in several physiological processes, inflammation-related disorders and cancer, their role in angiogenesis remains unclear. **Methods:** To elucidate the role of PADs in endothelial angiogenesis, we used two human EC models: primary vein (HUVECs) and microvascular endothelial cells (HMEC-1). PADs activity was inhibited using irreversible inhibitors: BB-CI-amidine, CI-amidine and F-amidine. We analyzed all three steps of angiogenesis *in vitro*: proliferation, migration, and capillary-like tube formation, as well as secretory activities, gene expression and signaling in ECs. **Results:** All used PAD inhibitors reduced the histone H3 citrullination (H3cit) mark, inhibited endothelial cell migration and capillary-like tube formation, and favored an angiostatic activity in HMEC-1 cells, by increasing PEDF (pigment epithelium-derived factor) and reducing VEGF (vascular endothelial growth factor) mRNA expression and protein secretion. Additionally, BB-CI-amidine reduced the total activity of MMPs (Matrix metalloproteinases). The observed effects were underlined by the

inhibition of Akt phosphorylation. **Conclusions:** Our findings suggest that pharmacological inhibitors of citrullination are promising therapeutic agents to target angiogenesis.

© 2024 The Author(s). Published by
Cell Physiol Biochem Press GmbH&Co. KG

Introduction

The human vasculature, formed through angiogenesis and vasculogenesis, is a vital regulator of body homeostasis through the mobilization of metabolites and catabolites, gas exchange, and inter-organ communication via the transport of hormones and other regulatory or immune-related factors [1]. Endothelial cells (ECs) lining the inner wall of arterial, venous, and microvascular vessels form the endothelium, which is now widely considered as a metabolically active and key endocrine organ.

The endothelium secretes a plethora of factors such as nitric oxide, von Willebrand factor, and vascular endothelial growth factors (VEGFs), which modulate blood flow, coagulation, pressure, and wound healing [2]. Angiogenesis, leading to the *de novo* formation of blood vessels from pre-existing ones, is considered a flagship function of ECs, which under physiological condition occurs during embryogenesis, wound healing, and the menstrual cycle [3]. Conversely, abnormal angiogenesis contributes to the etiology of many pathologies including cancer, tumor neovascularization [4], diabetic vascular complications [5], and obesity [6]. Among the mechanisms contributing to the shift from physiological to pathological endothelium, epigenetic alterations, including histone post-translational modifications (PTMs), may play an indispensable role, as aberrant histone acetylation is a signature of hyperglycemic damage in cultured aortic endothelial cells [7] and histone methylation acts as a signature of persistent glycemic damage [8].

A more recently discovered histone post-translational modification (PTM) is arginine citrullination, which in contrast to most histone PTMs such as methylation and acetylation, appears to be irreversible as its reversal can only be achieved by histone replacement [9]. The enzymatic conversion of peptidyl-arginines to citrulline is catalyzed by a conserved family of peptidylarginine deiminases (PADs) [10]. Replacement of the arginine primary ketamine group with the citrulline side chain ketone group leads to the loss of a positive charge [11]. The human “citrullinome” includes thousands of proteins [12] and notably histones [9]. Accumulating evidence suggests that histone citrullination, by modulating chromatin status, cellular metabolism, and gene expression, contributes to pathological processes including cancer progression [13] and inflammation [14]. Citrullination is widely regarded as an immune related histone PTM, as it was shown that aberrant levels of citrullination occur in several autoimmune mediated diseases, notably rheumatoid arthritis, and COVID-19 [15].

Mechanistically, citrullinated decondensed chromatin from neutrophils acts as a scaffold for the formation of the so-called neutrophil extracellular traps (NETs), a net-like structures enriched in bactericidal proteins [16, 17] whose formation can also be induced by reactive nitrogen molecules such as nitric oxide and peroxynitrite [18]. The release of decondensed chromatin and the formation of NETs contribute to thrombus formation [19] and mice deficient in PAD4 were shown to be protected from thrombus formation after experimental induction of venous stenosis [20]. Similarly, exposure of the endothelium to citrullinated histone H3, as found in NETs, contributes to microvascular endothelial barrier dysfunction through the opening of cellular adherens junctions and reorganization of the actin cytoskeleton of endothelial cells [21]. Conversely, a recent study showed that free citrullinated histones exert beneficial effects on endothelial cell function [22].

Although widely studied in immune cells, the effects of protein citrullination on the endothelium remain largely unknown, although recent results from several groups suggest that citrullination may influence vascular function. The aim of our study was to investigate, by pharmacological targeting, the contribution of PADs to endothelial cells proliferation, vascularization *in vitro*, wounding potential and explore the subjacent molecular mechanisms.

Materials and Methods

Cell culture

Human Microvascular Endothelial Cells (HMEC-1) were obtained from American Type Culture Collection (ATCC, Manassas, VA, USA). Human Umbilical Vein Endothelial Cells (HUVECs) were isolated from the veins of freshly collected umbilical cords, by collagenase type II digestion as described previously [23] and used for the experiments at passages 2-4. The study design and protocol involving the use of human umbilical cords were approved by the Bioethics Commission at the University of Lodz (Decision No. 15/KBBN-UŁ/III/2019 and 16 (III)/KBBN-UŁ/I/2021-22), all research was performed in accordance with relevant regulations and the guidelines of the Declaration of Helsinki. Informed consent was obtained from the donors at the Medeor Multidisciplinary Hospital in Lodz, no data regarding the donors were collected and stored, and the samples were completely anonymized. Both endothelial cell types were cultured in MCDB131 medium (Corning Life Sciences, Corning, NY, USA) supplemented with 10% fetal bovine serum (EurX, Gdansk, Poland), 10 ng/ml Epidermal Growth Factor (Millipore, Burlington, MA, USA), and 10 mM glutamine (Corning Life Sciences, Corning, NY, USA). For passaging and seeding, the cells were detached using 0.25% trypsin-EDTA solution (Corning Life Sciences, Corning, NY, USA).

PAD inhibitors used in the study

Three commercially available PAD inhibitors were used: BB-Cl-amidine (cat. no. HY-111347, MedChemExpress, Monmouth Junction, NJ, USA), Cl-amidine (cat. no. 506282, Merck, Darmstadt, Germany), and F-amidine (item no. 10610, Cayman Chemical Company, Ann Arbor, USA). All inhibitors were dissolved in DMSO (Chempur, Piekary Slaskie, Poland) according to the manufacturers' suggestions, aliquoted (to avoid freeze-refreeze cycles), and stored for up to 3 months according to the manufacturer's instructions. The final concentration of the solvent at the highest concentration of drugs did not exceed 0.6% of the volume sample and did not affect cellular metabolism, which was checked in the viability assay.

Cytotoxicity assay by resazurin reduction test

Cytotoxicity was analyzed by resazurin reduction to fluorescent resorufin, as described previously [24]. Cells were seeded onto 96-well plates at a density of 5,000 and 7,000 cells/well for HUVECs and HMEC-1 cells, respectively. After 16-20 h, the cells were treated with PAD inhibitors at a concentration range of 0.1-10 μM for 24 h. After the indicated time, the culture medium was removed, and cells were washed with phosphate buffered saline (PBS) containing $\text{Ca}^{2+}/\text{Mg}^{2+}$ and 5.5 mM glucose. The cells were then incubated for 2 h in the washing buffer supplemented with 0.0125 mg/ml resazurin. After incubation, fluorescence was read on a Fluoroscan Ascent microplate reader (Thermo Fisher Scientific, Waltham, MA, USA) at $\lambda_{\text{ex}} = 530 \text{ nm}$ and $\lambda_{\text{em}} = 590 \text{ nm}$.

Flow cytometry

Cell preparation for FACS analysis was based on a previously described method [25]. Briefly, ECs were plated on 6 cm dishes (ThermoFisher, Waltham, Massachusetts, USA), then after 16-20 h the cells were treated with PAD inhibitors. After 16 to 48 h of incubation, the cells were trypsinized, washed with PBS, and centrifuged for 5 min at $200 \times g$. For DNA content analysis, cells were fixed in 70% ethanol for 24 h at 4 $^{\circ}\text{C}$, centrifuged (10 min at $200 \times g$), washed with PBS, and centrifuged again (10 min at $200 \times g$). Cells were then resuspended in propidium iodide (PI) buffer containing RNase A (0.4 mg/ml; AppliChem, Darmstadt, Germany) and PI (5 $\mu\text{g}/\text{ml}$; ThermoFisher, Waltham, Massachusetts, USA) in PBS and incubated for 30 min. Nuclear DNA content was measured using an LSRII flow cytometer (Becton Dickinson, Franklin Lakes, NJ, USA). Flow acquisition was performed using FlowJo software (FlowJo, Williamson Way Ashland, USA).

RNA isolation, reverse transcription, and Real-Time PCR

Cells were plated onto 6-well plates (Thermo Fisher, Waltham, Massachusetts, USA) and after 16-20 h treated with PAD inhibitors for 16 h. Total cellular RNA was isolated and purified using an InviTrap Spin Cell RNA mini kit (Strattec Molecular, Birkenfeld, Germany) in accordance with the manufacturer's protocol. cDNA synthesis was performed using the PrimeScript RT Reagent Kit (Perfect Real Time, Takara, Japan) according to the manufacturer's instructions. Real-time polymerase chain reaction (real-time PCR) was performed using Eco Real-Time PCR (Illumina, San Diego, CA, USA). The final reaction volume was 10 μ L and contained: 0.2 nM of forward and reverse primers (Table 1 for sequences), cDNA template, SYBR Green (Perfect Real Time, Takara, Japan), and DNAase/RNAase-free water (46-000-CV, Corning Life Sciences, Corning, USA). The reactions were incubated at 96 °C for 2 min, followed by 40 cycles of 96 °C for 5 s and 60 °C for 30 s. *HPRT1* was used as a reference for gene expression normalization, performed according to the $2^{-\Delta\Delta Ct}$ method described by Livak [26].

Table 1. List of primers for quantitative PCR used in this study

Gene	Forward primer sequence 5'–3'	Reverse primer sequence 5'–3'
HPRT1	ATGGACAGGACRGAACGTCTT	TCCAGCAGGTCAGCAAAGAA
CCNA2	ACTGGTGGTCTGTGTTCTGTGA	GATGCCAGTCTTACTCATAGCTGAC
CCNB1	TGGTGAATGGACACCAAVTC	TAGCATGCTTCGATGTGGCA
CCND1	ATGCCAACCTCCTCAACGACC	TCTGTTCCCTCGCAGACCTCCA
CCNE1	CAGGGAGCGGGATGCG	GGTCACGTTTGCCTTCCTCT
CCNY	TGGCAGAAGCGAACAACCTG	AGGCGAGAGATGGCCTCAAG
VEGFA	CTACCTCCACCATGCCAAGT	ATGATTCTGCCCTCCTCCTT
VEGFC	CAGCAACACTACCACAGTGTCA	CTCCAGCATCCGAGGAAAACAT
SERPINE1	TGTCATAGTCTCAGCCCGCA	AAAAGGACTGTTCCCTGTGGGG
SERPINF1	GCGTATCCACAGGCCCCA	GGGCTGGCAGGGTTCTG
EDN1	GAGCTCCAGAAACAGCAGTC	TATCCATCAGGGACGAGCAG
IL6	CTCATTCTGCCCTCFAGCC	GACCGAAGGCGCTTGTGGA
IL8	ACCGGAAGGAACCATCTCAC	GGCAAACTFCACCTTCACAC
CCL2	TCTCAAACCTGAAGCTCGCACT	TGGGGCATTGATTGCATCTGG
VIM	TACCGGAGACAGGTGCAGT	CGTTCAGGGACTCATTGGTT
IGFBP2	GCTGGTCATGGGCGAGGG	TGGTCATCGCCATTGTCTGC
IGFBP3	CCTACCTGCTGCCAGCGCC	GGTGCGTGCTGGAGACGGAC
TIMP1	TGACATCCGGTTCGTCTACA	CTGCAGTTTTCCAGCAATGA

Western blotting

To determine the levels of PAD isoforms in ECs, HMEC-1 and HUVECs were seeded onto 60 mm dishes at 500, 000 cells/dish. After 24 h, total protein extract was prepared using Mammalian Protein Extraction Reagent (M-PER, ThermoFisher, Waltham, Massachusetts, USA) reagent according to the manufacturer's instructions. For histone citrullination assessments, cells were seeded onto 60 mm dishes (ThermoFisher, Waltham, Massachusetts, USA) at 2, 500, 000 cells/dish and after 18–20 h treated with PAD inhibitors and incubated for 16 h. Histone extracts were prepared following an acid extraction protocol as described previously [24]. For the study of Akt signaling, HMEC-1 were seeded onto 60 mm dishes at 500, 000 cells/dish and, after 18–20 h, treated with PAD inhibitors for 16 h. Total protein was prepared using Mammalian Protein Extraction Reagent (M-PER, ThermoFisher, Waltham, Massachusetts, USA) reagent according to the manufacturer's instructions. The extracts were immunoblotted to determine the level of citrullination of histone H3. 1 µg of histone extract or 10 µg of total protein extract was loaded onto polyacrylamide gels and resolved using Sodium dodecyl sulfate- Polyacrylamide gel electrophoresis (SDS-PAGE), then transferred to polyvinylidene fluoride (PVDF) membrane. The membrane was then washed with TBST buffer (10 mM Tris, pH 8.0, 150 mM NaCl, 0.5% Tween20) and blocked in 3% freshly prepared non-fat milk in Tris-buffered saline with Tween (TBST) overnight at 4 °C with agitation. After incubation, the membranes were washed thrice for 5 min each in TBST at room temperature. Next, the membranes were probed with primary antibodies prepared according to suppliers' instructions, for PAD expression: anti-PAD1 (dilution 1:1, 000; cat. no. ab181762, Abcam, Cambridge, UK), anti-PAD2, (dilution 1:1, 000; cat. no. ab16478, Abcam, Cambridge, UK), anti-PAD3 (dilution 1:1, 000; cat. no. sc-393622, Santa Cruz Biotechnology, Dallas, USA), anti PAD4 (dilution 1:1, 000; cat. no. ab128086, Abcam, Cambridge, UK) and β-actin (dilution 1:1, 000; cat. no. sc-69879, Santa Cruz Biotechnology, Dallas, USA) was used as loading control. For histone citrullination, H3R2R8R17cit (dilution 1:1, 000; cat. no. ab47915, Abcam, Cambridge, UK), H3 (dilution 1:1, 000; cat. no. ab18521; Abcam, Cambridge, United-Kingdom) was used as loading control. For PI3K/Akt signaling analysis: Pan-Akt (dilution 1:1000; cat. no. A18120, ABclonal, Woburn, USA), Phosphorylated-Akt S473 (dilution 1:000; cat. no. AP1208, ABclonal, Woburn, USA), PI3 Kinase p85 alpha (dilution 1:1000; cat. no. A4992, ABclonal, Woburn, USA), GSK3β (dilution 1:1000; cat. no. sc-81462, Santa Cruz Biotechnology, Dallas, USA), and the aforementioned β-actin antibody was used as a loading control. The membranes were incubated with primary antibodies overnight and then washed thrice with TBST for 5 min. The membranes were then incubated with horseradish peroxidase-conjugated secondary antibodies (dilution 1:10, 000, cat. no. 111007003 AffiniPure Fab Fragment Goat Anti-Rabbit IgG (H+L) and cat. no. 115-006-003 AffiniPure F(ab)2 Fragment Goat Anti-Mouse IgG (H+L), Jackson ImmunoResearch, Baltimore Pike, USA) for 1.5 h at room temperature. The signal from the membranes was visualized using ECL (ThermoFisher, Waltham, Massachusetts, USA) on the Azure 300 Chemiluminometer (Azure Biosystems, Sierra Trinity, USA).

Cytokines/chemokines/growth factors release assay

The release of selected angiogenesis-related proteins by endothelial cells was performed as previously described [27] using the Proteome Profiler Human Angiogenesis Array (R&D Systems, Minneapolis, USA). Cells were seeded onto 60 mm dishes at 3.5x10⁶ cells/dish and after 18–20 h treated with PAD inhibitors and incubated for 16 h. After incubation, the cell culture supernatants were collected, centrifuged, diluted, and mixed with a cocktail of biotinylated detection antibodies supplied by the manufacturer. The samples were then incubated overnight on a cytokine assay kit membrane. Following a wash to remove unbound material, streptavidin-HRP and chemiluminescent detection reagent were added to quantify protein levels. The signals from the membranes were visualized using an Azure 300 chemiluminometer (Azure Biosystems, Sierra Trinity, USA). The results were then analyzed and quantified using the Protein Array Analyzer tool in ImageJ (Rasband, W.S., ImageJ, U. S. National Institutes of Health, Bethesda, Maryland, USA, <https://imagej.nih.gov/ij/>), as described previously [28].

Matrix metalloproteinases (MMPs) activity kit

The total activity of MMPs in HMEC-1 cells treated with PAD inhibitors was measured using a fluorometric assay (MMP Activity Assay Kit, ab112146; Abcam, Cambridge, UK) according to the manufacturer's instructions. Briefly, HMEC-1 cells were seeded onto 6-well plates at a density of 700, 000 cells/well, followed by treatment with the highest concentration of all inhibitors. As a positive control

for MMP inhibition, 20 µg/ml doxycycline (DOX) was used. After 16 h, the supernatant was collected and incubated for 3 h with 2 mM 4-aminophenylmercuric acetate (APMA) to activate the MMPs. After that, the supernatants activated with APMA were transferred to a U-bottom 96-well plate, and MMP Green Substrate was added to the samples. Subsequently, fluorescence was read in all samples at 5-minute intervals using a Fluoroscan Ascent microplate reader (Thermo Fisher Scientific, Waltham, MA, USA) at $\lambda_{\text{ex}} = 490 \text{ nm}$ and $\lambda_{\text{em}} = 525 \text{ nm}$.

Capillary-like tube formation assay

Endothelial capillary tube-like formation was assessed using Matrigel (Corning Life Sciences, Corning, NY, USA) according to the manufacturer's instructions. A basement Matrigel membrane was diluted to a protein concentration of 5 mg/ml using a sterile medium MCDB131, that is, the same medium that we used for endothelial cell culture, and stored at $-20 \text{ }^{\circ}\text{C}$. Before the experiment, a sample of Matrigel was thawed (overnight at $4 \text{ }^{\circ}\text{C}$), plated onto 15-well plates (Ibidi, Martinsried, Germany), and incubated at $37 \text{ }^{\circ}\text{C}$ for 30-40 min to allow polymerization. Then, endothelial cells in the complete cell culture medium were seeded onto Matrigel-coated plates; HMEC-1: 3,000 cells/well, HUVECs 4,000 cells/well. After 6 h (for HMEC-1) or 8 h (for HUVECs), the created structures were stained with calcein-AM (ThermoFisher, Waltham, Massachusetts, USA) for 15 min. Endothelial cell capillary tubes were assessed by fluorescence and phase contrast microscopy (Nikon Eclipse TE200 microscope, Tokyo, Japan) with a Zeiss CCD video camera (AcioCamERc5s, Oberkochen, Germany). The characterization of the created structures was performed by measuring the number, length, and width of the capillary tubes using the Angiogenesis Analyzer tool in ImageJ (Rasband, W.S., ImageJ, U. S. National Institutes of Health, Bethesda, Maryland, USA, <https://imagej.nih.gov/ij/>) [29].

Wound healing assay

Cells were seeded in 24-well plates at a density of 400,000 cells/well. After overnight incubation, cells were pretreated with PAD inhibitors for 16 h before scratching the confluent monolayer. To exclude the influence of endothelial cells proliferation on wound closure, the medium was supplemented with the cytostatic agent mitomycin C (at a final concentration of 10 µg/ml; Sigma-Aldrich, Saint Louis, MO, USA) throughout the experiment. Next, the cells were incubated in inhibitor-free medium, and after 8 h, the size of the wound was measured. Cell migration was tracked using a phase-contrast microscope image analysis system (Nikon Eclipse TE200 microscope, Tokyo, Japan) with a Zeiss CCD video camera (AcioCamERc5s, Oberkochen, Germany). Wound healing inhibition analysis was performed using the Wound Healing Tool plugin in ImageJ (Rasband, W.S., ImageJ, U. S. National Institutes of Health, Bethesda, Maryland, USA, <https://imagej.nih.gov/ij/>) [30].

Statistical analysis

Statistical analysis was performed using GraphPad Prims 9.0 (GraphPad, San Diego, California, USA). Normality in the data distribution was determined using the Kolmogorov-Smirnov test. Differences between groups were assessed by the one-way ANOVA and post hoc analysis by Dunnett's test was performed. Significance of the results is indicated on the graphs (*** <0.0001 , ** <0.001 , * <0.05), and all the results are shown for the treated condition vs control.

Results

The expression of PAD isoforms renders ECs susceptible to PAD inhibitors

We initially assessed the protein expression levels of PAD isoforms – PAD1, PAD2, PAD3 and PAD4 – in microvascular HMEC-1 and macrovascular HUVECs cells (Fig. 1A) and observed easily detectable PAD proteins levels in both cell types. Next, we tested the cytotoxicity of three PAD inhibitors, BB-Cl-amidine (BBCLA, 0.25 – 5 μM range), Cl-amidine (CLA, 0.25 – 10 μM range) and F-amidine (FA, 0.25 – 10 μM range) on both cell lines. BBCLA, which displays highest inhibitory potency towards several PAD isoforms (Table 2), exerted a cytotoxic effect with a half-maximal inhibitory concentration (IC_{50}) of 1.75 μM and 1.97 μM for HMEC-1 and HUVECs, respectively (Fig. 1B and 1D). Conversely, CLA and FA showed no major effects on cellular viability at the tested concentrations (Fig. 1B and 1D). We also investigated the effects of higher concentrations of CLA and FA and observed no cytotoxic effects up to 100 μM (data not shown). Next, PAD inhibitors were tested for biochemical inhibitory potency, which was assessed by analyzing histone H3 citrullination levels (H3Cit) (Fig. 1C and 1E). Given the high cytotoxicity of BBCLA, concentrations of 0.25, 0.5, and 1 μM were used. For both CLA and FA, concentrations of 2, 5 and 10 μM were selected. BBCLA was the most potent PAD inhibitor in both endothelial cell models, reducing histone citrullination more than 4-fold (Fig. 1C and 1E) at the highest concentration (1 μM). The inhibitory activity of CLA closely followed that of FA, lowering the H3cit mark by almost 3-fold in both EC models at the highest concentration. These data indicate that a high inhibition of H3cit is cytotoxic, while milder inhibition, halving H3Cit levels, may affect endothelial cell function without toxic effects.

Table 2. Summary of the biochemical properties of the inhibitors used in this study

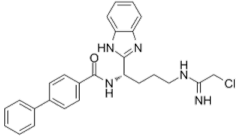
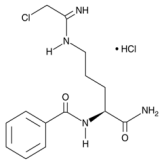
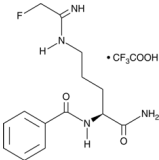
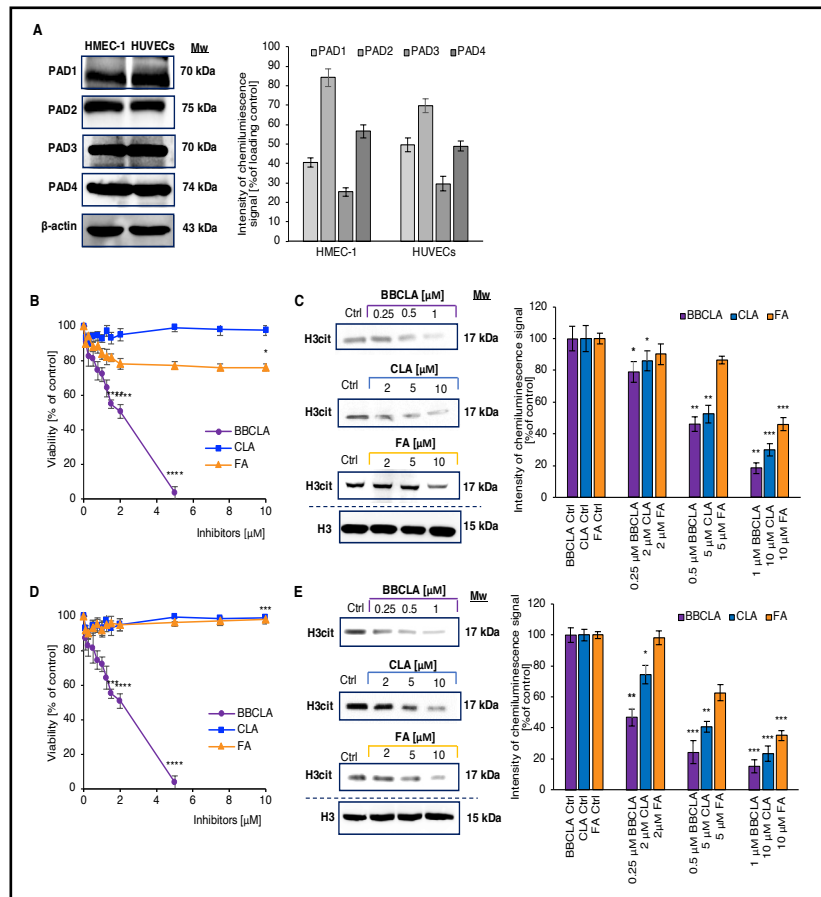
Inhibitor	BB-Cl-amidine	Cl-amidine	F-amidine
IUPAC name and molecular weight (MW)	N-[(1S)-4- [(1-amino-2 chloroethylidene) amino]-1-(1H-benzimidazol-2-yl) butyl]-4-phenylbenzamide MW = 459.97	N-[(2S)-1-amino-5-[(1-amino-2-chloroethyl-idene) amino]-1-oxopentan-2-yl] benzamide MW = 310.78	N-[(2S)-1-amino-5- [(1-amino-2-fluoroethyl- idene) amino]-1-oxopentan-2-yl] benzamide MW = 294.32
Chemical formula			
In vitro inhibitory potency against PADs (target and K_i)	k_{inact}/K_i PAD1 = 16 100 $\text{M}^{-1} \text{min}^{-1}$ k_{inact}/K_i PAD2 = 4 100 $\text{M}^{-1} \text{min}^{-1}$ k_{inact}/K_i PAD3 = 6 800 $\text{M}^{-1} \text{min}^{-1}$ k_{inact}/K_i PAD4 = 13 300 $\text{M}^{-1} \text{min}^{-1}$	k_{inact}/K_i PAD1 = 37,000 $\text{M}^{-1} \text{min}^{-1}$ k_{inact}/K_i PAD2 = 1200 $\text{M}^{-1} \text{min}^{-1}$ k_{inact}/K_i PAD3 = 2000 $\text{M}^{-1} \text{min}^{-1}$ k_{inact}/K_i PAD4 = 13,000 $\text{M}^{-1} \text{min}^{-1}$	k_{inact}/K_i PAD1 = 2800 $\text{M}^{-1} \text{min}^{-1}$ k_{inact}/K_i PAD2 = 380 $\text{M}^{-1} \text{min}^{-1}$ k_{inact}/K_i PAD3 = 170 $\text{M}^{-1} \text{min}^{-1}$ k_{inact}/K_i PAD4 = 3000 $\text{M}^{-1} \text{min}^{-1}$
Inhibitory mechanism	Covalent modification of the active site residue Cys645 ²⁹		
Potential off-target effects on endothelial cells	Cytotoxicity at > 1 μM on both HUVEC and HMEC	Minor at the concentrations used in this study	Minor at the concentrations used in this study

Fig. 1. Expression of selected PAD isotypes in endothelial cells and the effect of their inhibition on cell viability and histone citrullination levels (abbreviations; Ctrl; Experimental control, BBCLA - BB-Cl-amidine, CLA - Cl-amidine, FA - F-amidine). A. Western blot analysis of PAD isoforms levels in ECs, representative blots from three independent experiments are shown, the chart visualizes densitometry of the chemiluminescence signal calculated vs loading control; B, D. Viability of endothelial cells treated with PAD inhibitors for 24 h: B. HMEC-1, D. HUVECs. Data are presented as mean \pm SD (n = 5). Statistics: One-way ANOVA control vs. treated, post-hoc Dunnett's test, sample vs. control (**<math><0.0001</math>, **<math><0.001</math>, *<math><0.05</math>). C, E.



Levels of histone citrullination in ECs treated with PAD inhibitors for 16 h. C. HMEC-1, E. HUVECs. The presented western blots are representative of three independent experiments, and the charts visualize densitometry of the chemiluminescence signal calculated vs. loading control, presented as mean \pm SD (n = 3). Statistics: one-way ANOVA control vs. treated, post-hoc Dunnett's test, sample vs. control (**<math><0.0001</math>, **<math><0.001</math>, *<math><0.05</math>).

No significant effect of PAD inhibition on ECs cell cycle

No significant changes for the selected inhibitor concentrations were observed in a resazurin proliferation assay (Fig. 2B). A statistically significant effect on endothelial cell proliferation was observed only at higher concentrations of BBCLA (>1 μ M), which were not used in subsequent experiments, and no significant results were obtained for either CLA or FA in the tested concentration range. HMEC-1 cells were treated with nontoxic concentrations of PAD inhibitors for several incubation times (16, 24, 32, and 48 h). HMEC-1 cells were treated with nontoxic concentrations of PAD inhibitors for several incubation times (16, 24, 32, and 48 h). Flow cytometry analysis showed no significant differences in the cell cycle progression of PAD inhibitor-treated HMEC-1 cells (Fig. 2C and D). A minor increase in the number of cells in the G₁ phase was detected after 16 h (Fig. 2C and D). Conversely, PAD inhibition significantly altered the expression profile of several cyclins in an incubation time dependent manner (Fig. 2A). Most notably, cyclin E (CCNE) and cyclin D (CCND) were found to be significantly decreased by all inhibitors after 16 h. Although the change in cyclin expression profile was not sufficient to alter the cell cycle of PAD inhibitor-treated HMEC-1 cells, the change in CCNE and CCND expression may be responsible for the slight increase in the percentage of cells in the G₀/G₁ phase after 16 h.

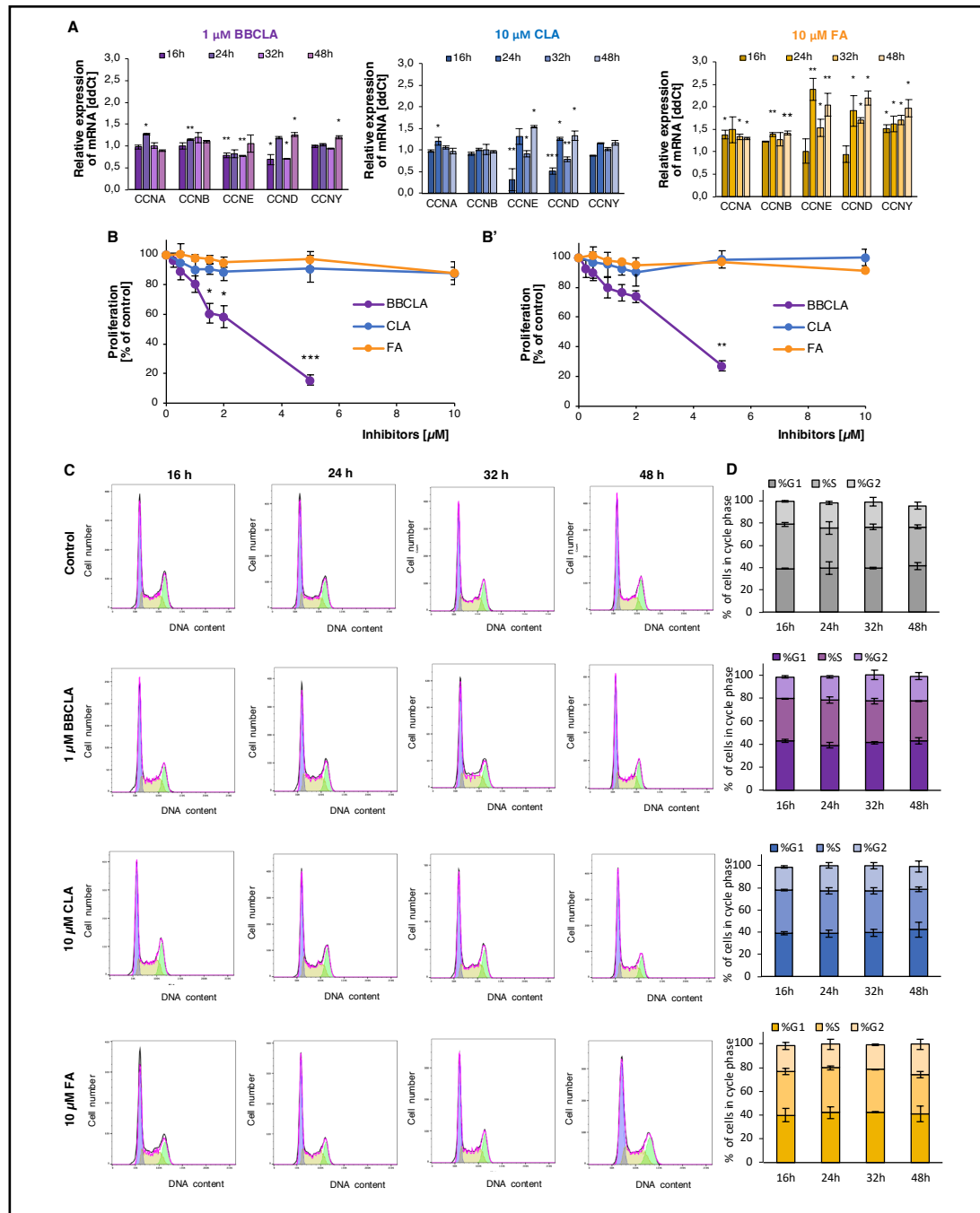


Fig. 2. A. Cyclin mRNA expression profile in PAD inhibitor-treated HMEC-1 over a time-course incubation time 16-48h. Data are presented relative to untreated cells. Statistics: One-way Anova control vs. treated, post-hoc Dunnett's test, sample vs. control ($***<0.0001$, $**<0.001$, $*<0.05$). B. Proliferation of HMEC-1 (B) treated with PAD inhibitors for 48 h. Data are presented as mean \pm SD (n = 3). Statistics: One-way ANOVA, control vs. treated, post-hoc Dunnett's test, sample vs. control ($***<0.0001$, $**<0.001$, $*<0.05$). B'. Proliferation of HUVECs cells treated with PAD inhibitors for 48 h. Data are presented as mean \pm SD (n = 3). Statistics: One-way ANOVA, control vs. treated, post-hoc Dunnett's test, sample vs. control ($***<0.0001$, $**<0.001$, $*<0.05$). C. Cell cycle progression in PAD inhibitor-treated ECs. A. Flow cytometry plots from HMEC-1 cells treated with PAD inhibitors for 16, 24, 32 or 48 h. DNA was stained using propidium iodide/RNaseA solution. Representative plot from each time point is shown (n = 3). D. Percentage of HMEC-1 cells in each phase of the cell cycle at each incubation time, analyzed by propidium iodide flow cytometry staining, and presented as mean \pm SD (n = 3). Statistical analysis was performed using ANOVA and post-hoc Dunnett's test, sample vs. control

Pharmacological inhibition of PADs affects in vitro capillary tube formation and „wound healing” in HMEC1 and HUVECs

Subsequently, we used selected PAD inhibitor concentrations to investigate the contribution of protein citrullination to the regulation of angiogenesis-like responses in our *in vitro* EC models. As pharmacological inhibition of PADs affected cell viability and proliferation of endothelial cells, we analyzed the response of HMEC1 and HUVECs cells to PAD inhibitors in terms of angiogenic potential by performing the capillary-tube formation assay (Fig. 3) and cell migration assay (Fig. 4). The inhibition of PADs by the three different inhibitors affected the organization and several morphological parameters of the capillary net. Inhibitory effects on tube formation were observed in both HMEC-1 cell lines (Fig. 3A) and HUVECs (Fig. 3B), with stronger de-structuring of capillary tube formation by BBCLA compared to CLA and FA in HMEC-1 and no significant results for FA in HUVECs.

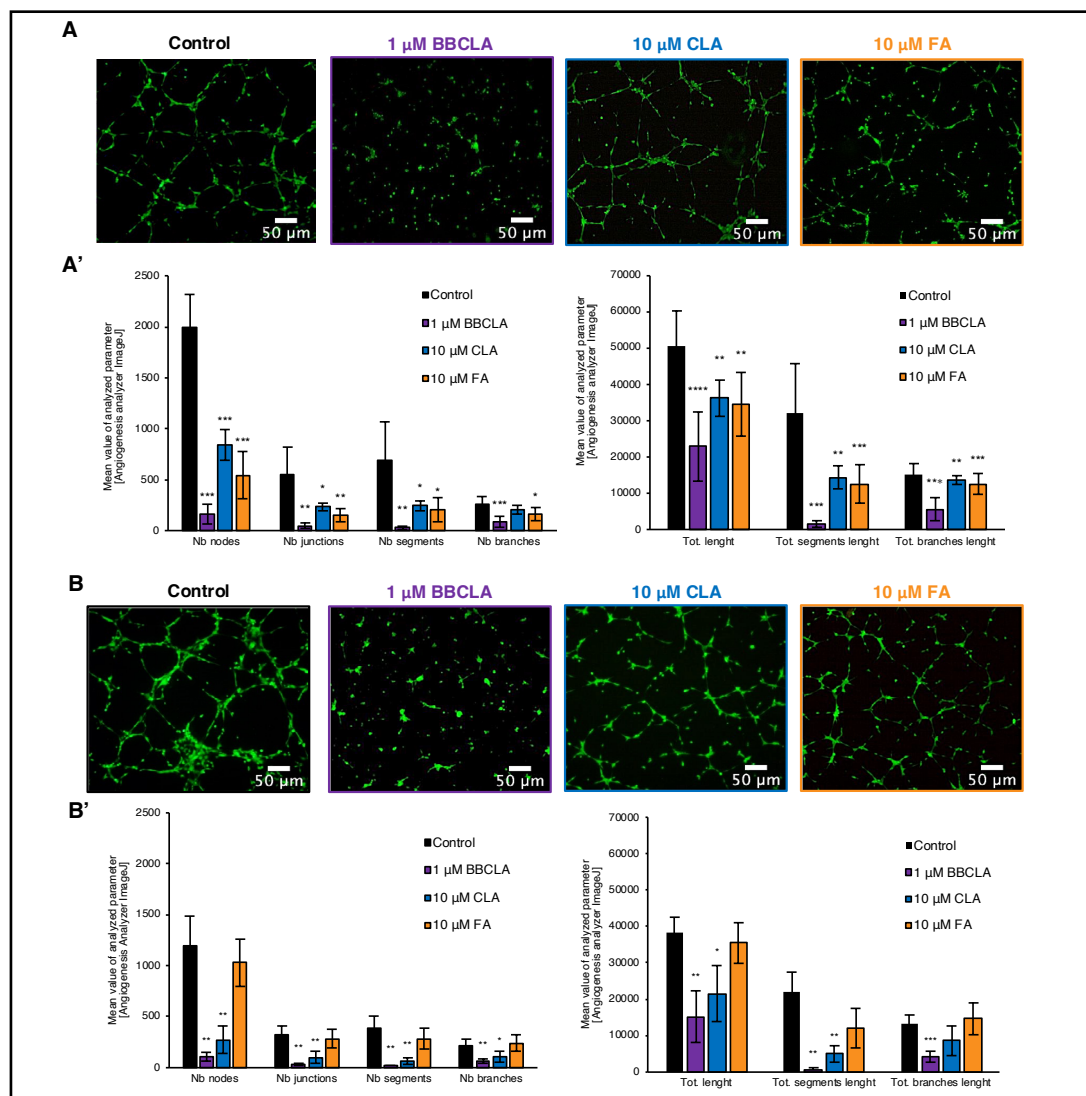


Fig. 3. Inhibition of capillary-like tube formation by PADs inhibitors in HMEC-1 and HUVECs in Matrigel matrix (Abbreviations: Nb, number; Tot. - Total). A. HMEC-1 and B. HUVECs panels containing representative pictures of BBCLA, CLA and FA treatments on the formation of the capillary-like structures stained with Calcein-AM, magnification 4x. Images are representative of five independent experiments. A'. and B'. show the analysis of the parameters characterizing capillary-like structures after PAD inhibition in HMEC-1 and HUVECs endothelial cells respectively. Data are presented as mean \pm SD, n = 9. Statistics: one-way ANOVA control vs. treated, post-hoc Dunnett's test (*** <0.0001 , ** <0.001 , * <0.05).

Next, we monitored endothelial cell migration potential. In both HMEC-1 and HUVECs, cell migration, as seen by the filling of the “wounded” area after 8 h, was almost complete in vehicle-treated cells (Fig. 4). Conversely, significantly reduced cell migration was observed upon pre-incubation with the BBCLA, CLA and FA, with a slightly stronger effect of BBCLA (Fig. 4A', 4B'). Thus, inhibition of PADs suppressed the migration of HMEC-1 and HUVECs into cell-free areas. Overall, pharmacological inhibition of PADs destabilizes capillary-like tube formation and cell migration, which are two processes necessary for angiogenesis.

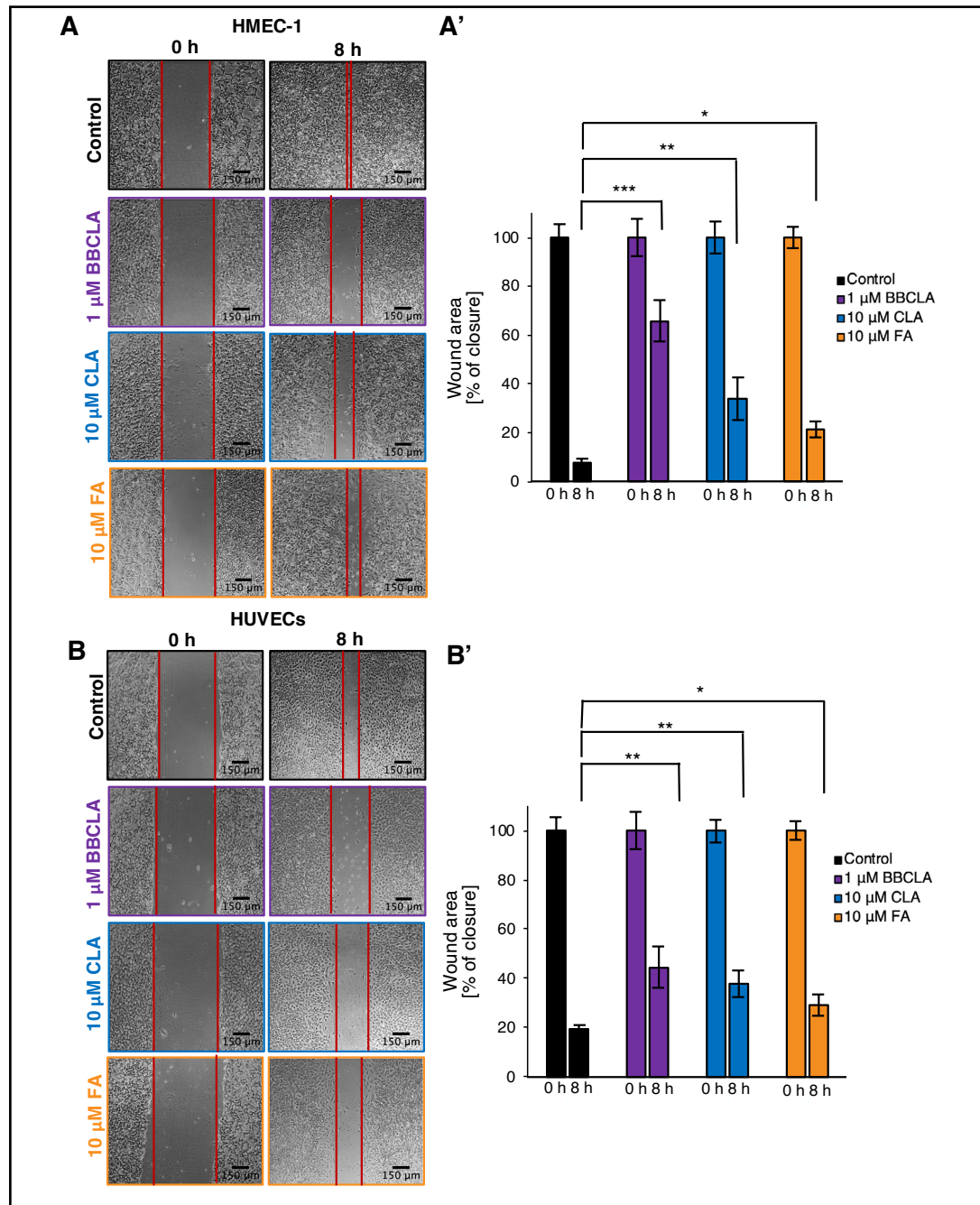


Fig. 4. Inhibition of PADs activity in endothelial cells inhibited cell migration in a wound-healing assay. Cells were pretreated with PAD inhibitors for 16 h before creating a scratch in the confluent monolayer. Next, the cells were incubated in inhibitor-free medium, and after 8 h, the size of the wound was measured. A, B. Representative phase-contrast images of HMEC-1 cells and HUVECs taken at 0 and 8 h post-scratch, magnification 10x. A', B'. Wound healing area analysis was performed using the Wound Healing Tool plugin in ImageJ. Data are presented as mean ± SD. Statistics: one-way ANOVA control vs. treated (***<0.0001, **<0.001, *<0.05).

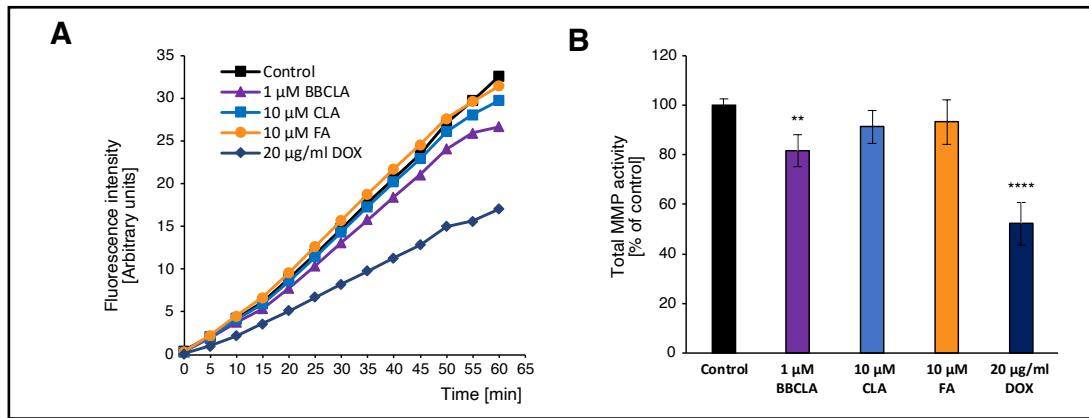


Fig. 5. Total MMP activity in PAD inhibitor treated HMEC-1. A. Kinetic graph of total MMP activity in HMEC-1 treated with PAD inhibitors for 16 h, in relative fluorescence intensity units over 60 min with 5 min measurement interval. B. Total MMP activity in HMEC-1 cells treated with PAD inhibitors for 16 h, data presented as percentage of control, mean \pm SD (n = 3). Statistics: one-way ANOVA control vs. treated, post-hoc Dunnett's test (**** <0.0001 , ** <0.001 , * <0.05).

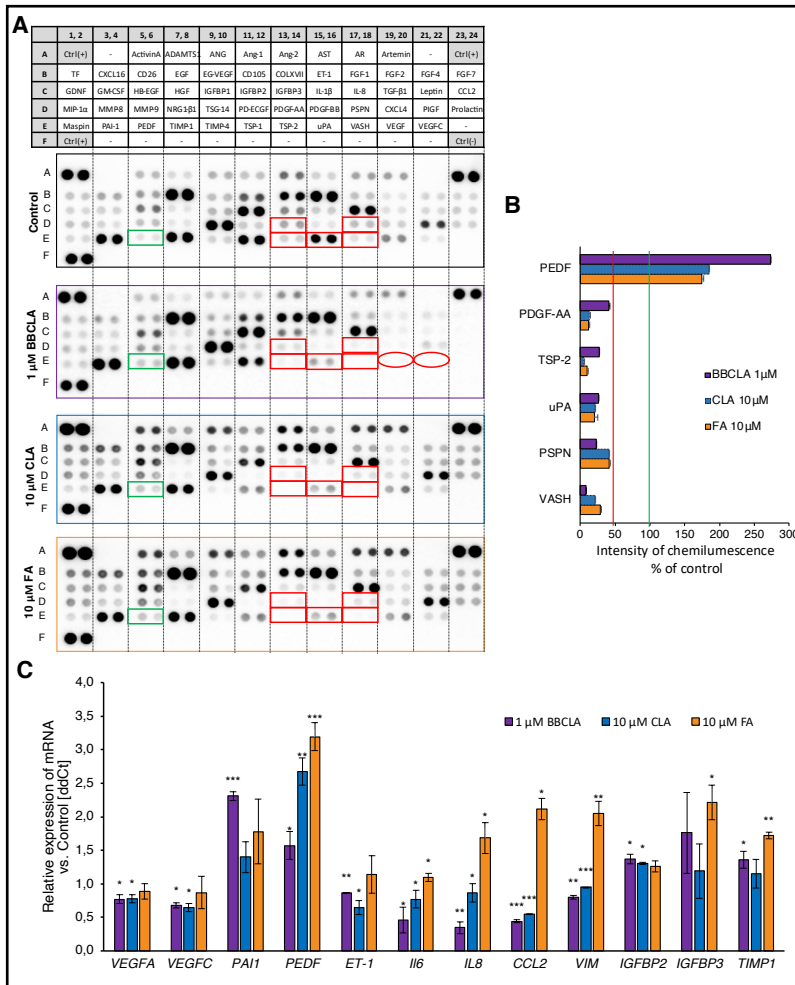
With the results of PAD inhibition on ECs capillary formation and migration we monitored the activity of the MMPs one of the key players in the analyzed angiogenesis processes. We found that the total MMP activity was significantly lowered in the HMEC-1 upon 16 h incubation with 1 μ M BBCLA (Fig. 5A, B). However, no significant reduction in enzyme activity was observed upon 10 μ M CLA and 10 μ M FA treatment.

PADs inhibitors induce an anti-angiogenic profile in HMEC-1 and affect Akt activation

To evaluate the effects of PAD inhibitors on ECs functions, we analyzed the secretory profile of HMEC-1 treated with inhibitors for 16 h. Fig. 5A shows the signals of the secreted cytokines, chemokines, and growth factors released in the conditioned medium in response to PADs inhibitors. Among the most prominent features, we detected decreased secretion of Vascular Endothelial Growth Factor A (VEGFA) and Vascular Endothelial Growth Factor C (VEGFC) upon BBCLA treatment of HMEC-1 to 5% and 11% of the control, respectively. We have highlighted these significant changes in the appropriate representative dot-blot membranes (Fig. 6A, B). In the case of the other two inhibitors, VEGFs downregulation was milder. CLA: 81% for VEGFA and 62% for VEGFC; FA: 49% for VEGFA and 42% for VEGFC (Fig. 6A, B). These results were then verified at the transcriptional level, and we found that BBCLA and CLA, but not FA treatment, significantly reduced *VEGFA* and *VEGFC* mRNA expression. In addition, we detected increased serpinE1 (PAI1) and serpin F1 (PEDF) levels (Fig. 6A, B), which was also supported by concordant changes in the expression levels of the respective genes (Fig. 6C). Overall, the modulation of the secretion pattern was almost coincident with CLA and FA, whereas BBCLA also displayed specific modulation of endothelial cells. We also found several inflammatory genes downregulated in BBCLA- and CLA-treated HMEC-1 cells, namely Interleukin-6 (*IL6*), Interleukin-8 (*IL8*), and C-C Motif Chemokine Ligand 2 (*CCL2*) with an opposite effect in FA-treated cells (Fig. 6C).

Given the multiple anti-angiogenic responses observed upon PAD inhibitor treatment, we monitored the activation status of PI3K-Akt signaling (Fig. 7). In HMEC-1 cells treated for 16 h with the three PAD inhibitors, the expression levels of the key PI3K-Akt signaling enzymes, total Akt, PI3K p85 adapter subunit were not affected by inhibitor treatment, and glycogen synthase kinase 3 β (GSK3 β) was only mildly downregulated by FA (Fig. 7A and 7B). In contrast, the activation status of the PI3K-Akt signaling pathway was inhibited by the three inhibitors, as Akt phosphorylation at Ser473 was reduced by >60% (Fig. 7A and 7B). Thus, PI3K-Akt signaling may be a downstream target of PAD inhibition. In Fig. 8, we propose a mechanism for the observed anti-angiogenic profile of endothelial cells treated with PAD inhibitors.

Fig. 6. Release of angiogenesis-related molecules from HMEC-1 treated with PAD inhibitors for 16 h. A. Representative images of dot blot membranes from the Angiogenesis Array. Green rectangles, proteins upregulated by more than 50% by all inhibitors; red rectangles, proteins downregulated by more than 50% by all inhibitors; circles, proteins downregulated by BBCLA only. B. Quantification of the chemiluminescent signal of each membrane spot from PAD inhibitor-treated cell membranes is presented as mean percentage of control membrane, mean + SD (n = 2). (Abbreviations for A, B: TF – Tissue Factor; GDNF – Glial Cell Derived Neurotrophic Factor; MIP-1 α – Macrophage Inflammatory Protein 1; MASPIN – Serpin Family B Member 5; CXCL16 – C-X-C



Motif Chemokine Ligand 16; GM-CSF – Granulocyte Macrophage Colony Stimulating Factor; PAI-1- Serpin Family E Member 1; INHBA – Inhibin Subunit Beta A; DPPIV – Dipeptidyl peptidase-4; HB-EGF – Heparin Binding EGF Like Growth Factor; PEDF – Serpin Family F Member 1; ADAMTS1 – ADAM Metallopeptidase With Thrombospondin Type 1 Motif 1; EGF – Epidermal Growth Factor; HGF – Hepatocyte Growth Factor; NRG1- β 1 – Neuregulin 1; TIMP1 – TIMP Metallopeptidase Inhibitor 1; ANG – Angiogenin; EG-VEGF – Endocrine gland-derived vascular endothelial growth factor; IGFBP1 – Insulin Like Growth Factor Binding Protein 1; TSG-14, tumor necrosis factor-stimulated gene 14 (also known as PTX3 – Pentraxin 3); TIMP-4 – TIMP Metallopeptidase Inhibitor 4; Ang-1 – Angiopoietin 1; CD 105 – Endoglin; IGFBP2 – Insulin Like Growth Factor Binding Protein 2; PD-ECGF – Platelet-derived Endothelial Cell Growth Factor; TSP1 – Thrombospondin 1; Ang-2 – Angiopoietin-2; IGFBP3 – Insulin Like Growth Factor Binding Protein 3; PDGF-AA – Platelet Derived Growth Factor Subunit A; TSP2 – Thrombospondin 2; AST – Angiostatin; ET-1 – Endothelin 1; IL-1 β – Interleukin 1 Beta; PDGF-AB – Platelet Derived Growth Factor Subunit B; uPA – Plasminogen Activator, Urokinase; AR – Amphiregulin; FGF-1 – Fibroblast Growth Factor 1 acidic; IL-8 – Interleukin 8; PSPN – Persephin; VASH1 – Vasohibin 1; FGF-2 – Fibroblast Growth Factor 2 basic; TGF- β 1 – Transforming Growth Factor Beta 1; CXCL4 – Platelet Factor 4; VEGFA – Vascular Endothelial Growth Factor A; FGF4 – Fibroblast Growth Factor 4; PIGF – Placental growth factor; VEGFC – Vascular Endothelial Growth Factor C; FGF-7 – Fibroblast Growth Factor 7; MCP1 – Monocyte Chemoattractant Protein-1.) C. Expression of angiogenesis and inflammatory genes in HMEC-1 after 16h of incubation with PAD inhibitors vs. untreated control normalized to the expression of HPRT1; data are presented as mean \pm SD (n = 3). Statistics one-way ANOVA control vs. treated, post-hoc Dunnett's test (***<0.0001, **<0.001, *<0.05).

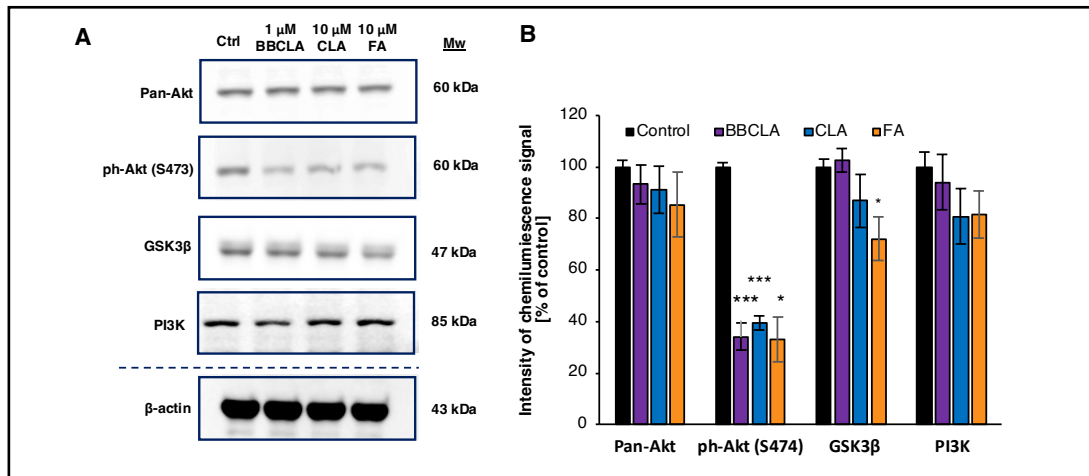


Fig. 7. Inhibition of Akt phosphorylation in HMEC-1 cells treated with PAD inhibitors for 16 h. A. Representative immunoblot of total Akt (Pan-Akt), phosphorylated Akt (on Ser 473), PI3K adapter subunit p85 and GSK3β in HMEC-1 cells treated with the indicated PAD inhibitors (BBCLA, CLA, and FA) for 16 h. B. Quantification of Pan-Akt, phosphorylated Akt, PI3K and GSK3β immunoblotting signals calculated using β-actin as loading control, the signal of ph-Akt(S474) was normalized to the level of Pan-Akt. Data are presented as mean ± SD (n = 3). Statistical analysis was performed using one-way ANOVA, post-hoc Dunnett's test (***<0.0001, **<0.001, *<0.05).

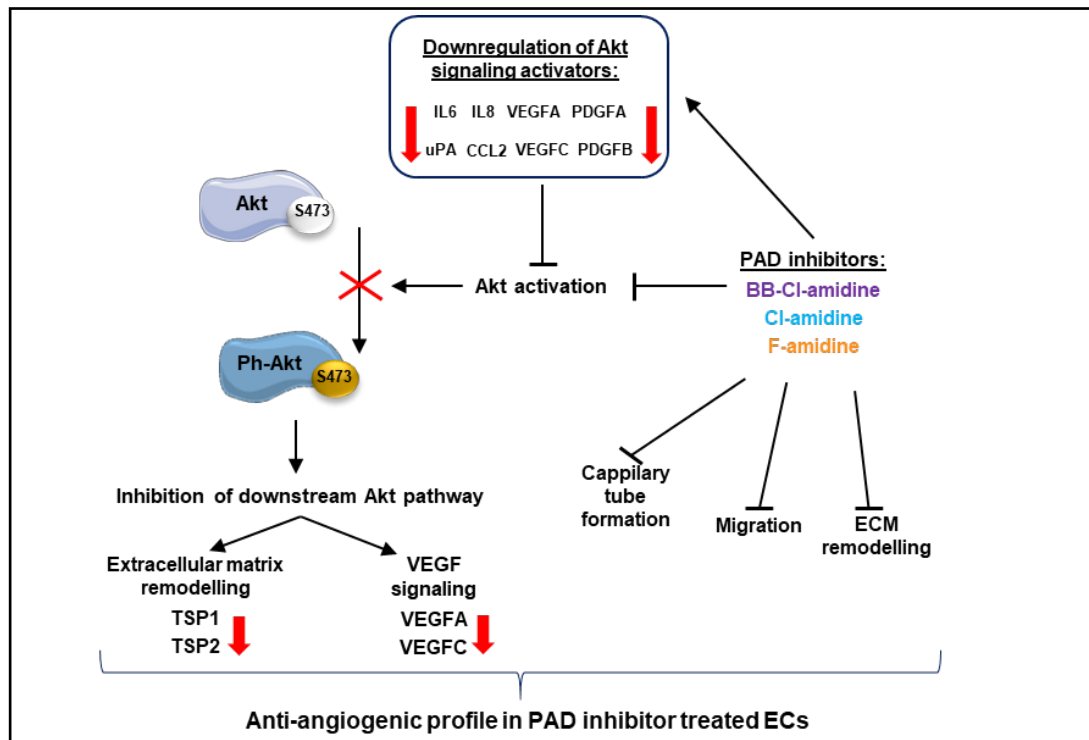


Fig. 8. Proposed mechanism of action of PAD inhibitors in the alteration of Akt signaling and modulation of the angiogenic potential of ECs. (Abbreviations: Akt - protein kinase B, Ph-Akt - phosphorylated protein kinase B; CCL-2 - Monocyte Chemoattractant Protein-1(MCP1); ECM- extracellular matrix; IL6, 8 - Interleukin 6, 8; PDGFA, PDGFB - Platelet Derived Growth Factor Subunit A, Subunit B; TSP1, 2 - Thrombospondin 1, 2; uPA - Plasminogen Activator; VEGFA, C - Vascular Endothelial Growth Factor A, C.

Discussion

Endothelial cells play a foundational role in vascular biology, influencing development, repair, and the maintenance of homeostasis within the cardiovascular system. Their functions are regulated by multiple stimuli and signaling pathways. In our study, we specifically explore the role of protein citrullination in endothelial cell function. By employing pharmacological approaches, we demonstrate that the inhibition of PADs affects endothelial cells proliferation, *in vitro* capillary tube formation and wound healing. Furthermore, PADs inhibitors extensively altered the endothelial cells secretion of multiple cytokines and angiogenic factors, defining citrullination as a PTM contributing to the regulation of endothelial cells biology. In recent years, numerous angiostatic molecules have been identified as target enzymes involved in the determination of histone PTMs patterns, such as histone deacetylases (HDACs) and histone methyltransferases (HMTs) [31], suggesting a promising strategy to inhibit endothelial proliferation. Our previous works demonstrated that broad inhibition of arginine and lysine methyltransferases suppresses angiogenesis [32] and the specific inhibition of G9a HMT suppresses the proliferation of human microvascular endothelial cells [33].

Using the immortalized microvascular (HMEC-1) and primary macrovascular (HUVECs) endothelial cells, as the experimental models, we found that both cell types express noticeable amounts of the PAD isoforms PAD1, 2, 3, and 4 at the protein level (Fig. 1A). Incubation of cells with the PAD inhibitor – BBCLA led to strong inhibition of cell viability, with an IC_{50} of approximately 2 μ M BBCLA. In contrast, CLA and FA treatments did not affect cell viability at concentrations of up to 10 μ M (Fig. 1B, D). The observed cytotoxic effect of BBCLA may be linked to its different chemical structure and longer *in vivo* half-life compared to CLA and FA, additionally BBCLA was also found to be almost 20-fold more cytotoxic than CLA to U2OS cells [10]. Upon treatment of endothelial cells with CLA, FA (up to 10 μ M), and BBCLA (up to 1 μ M to exclude cytotoxic effects of the inhibitor), the three inhibitors effectively inhibited histone H3 arginine citrullination by > 50% at the highest concentrations tested (Fig. 1C, E). PADs inhibitors affected the proliferation machinery, altering the expression profile of selected cyclins and notably lowering *CCNE* and *CCND* after 16 h (Fig. 2A/B). However, no significant changes in cell cycle progression were observed during the 16, 24, 32, and 48 h inhibition periods by flow cytometry, with only a slight but non-significant increase in G_0/G_1 percentage of cells after 16 h of treatment with PAD inhibitors (Fig. 2C, D). Recent data from nasopharyngeal carcinoma cells suggest that PAD4 promotes cell cycle progression, as its overexpression lowers the percentage of cells in the G_0/G_1 phase [34].

Next, we examined the effects of PAD inhibition on the angiogenic potential of ECs using standard assays. Using a Matrigel™-based assay, we studied the generation of capillary-like structures by HMEC-1 with different measurable features, including the number and length of nodes, junctions, segments, and branches, which were significantly inhibited by the three inhibitors (Fig. 3A, A'). Similarly, inhibition of capillary-like structures formation was observed in HUVECs (Fig. 3B, B'). The three inhibitors also prevented cell spreading in a „wound healing” assay (Fig. 4). Given these findings, and to study the possible underlying mechanisms, we analyzed the total activity of MMPs in HMEC-1 cells treated with PAD inhibitors for 16 h (Fig. 5). We observed that only 1 μ M BBCLA significantly lowered the total MMPs activity, which may in part explain the strong anti-angiogenic effects on ECs treated with this compound, as MMPs are crucial for extracellular matrix (ECM) reorganization during both capillary formation and cell migration [35, 36]. We then analyzed the release of chemokines, cytokines, and angiogenic factors into the culture medium, and we observed extensive changes upon incubation of HMEC-1 cells with PADs (Fig. 6). In keeping with the reduced *in vitro* formation of a capillary network and reduced wound healing, PAD inhibitor-treated HMEC-1 cells displayed reduced secretion of angiogenic factors VEGFA and VEGFC. Furthermore, 1 μ M BBCLA induced secretion and increased mRNA expression of *PAI-1* in HMEC-1 (Fig. 6A, 6C), which is involved in the regulation of blood coagulation and is reported

to be inactivated by citrullination [37]. As citrullinated serpins contribute to pathological thrombus formation in several autoimmune conditions, including rheumatoid arthritis, multiple sclerosis, and ulcerative colitis [38], PAD-induced inhibition of serpine citrullination, although not investigated in this study, may also contribute to endothelial health. Also, it has recently been shown that exogenously added PAI-1 inhibits angiogenesis *in vivo* [39]. Moreover, the secretion of uPA, a molecule that plays a role in the proteolytic degradation of the ECM [40], was decreased by each PAD inhibitor. As PAI-1 functions as a uPA inhibitor, its increased secretion coupled with decreased uPA levels may significantly lower the ability of ECs to modulate the ECM, thereby inhibiting angiogenesis. In addition, all the PAD inhibitors used in this study convergently upregulated PEDF (Serpin F1) secretion (up to almost 300% and 200% of the control for BBCLA and CLA/FA, respectively) and *PEDF* mRNA expression in HMEC-1 (Fig. 6A, 6C). *In vitro* mouse studies showed that PEDF inhibited migration and tube formation by dermal microvascular endothelial cells, consistent with the results of our study on human ECs [41, 42].

As PAD activity is strongly linked to inflammation, we also report that PAD inhibition by BBCLA and CLA downregulated the expression of *IL-6*, *IL-8*, *VIM*, and *CCL2* in HMEC-1 cells (Fig. 6C). In contrast, FA treatment increased the expression of these factors, a phenomenon that requires further insight and may be an effect of different substrate specificity of the inhibitors, the lower inhibitory potential of FA or an off-target effect of the compound. It cannot be excluded that the strong anti-angiogenic profile of BBCLA-treated HMEC-1 may also be related to the significant lowering of *CCL2* and *IL8* expression, strong pro-angiogenic factors that are also reported to regulate the expression of VEGF [43]. Studies performed on peripheral blood cells have shown that citrullination of histone H3 arginine 8 (H3R8), driven by PAD4, is required for the expression of IL-8 and other immune genes such as TNF-alpha [44]. Vimentin is one of the best studied PAD substrates, and functions as a pro-angiogenic molecule [45] and in our study it was also downregulated by BBCLA and CLA. Although we have discussed the citrullination of several angiogenesis-related proteins, such as serpins and vimentin, the human citrullinome may encompass hundreds of either anti- or pro-angiogenic molecules that require citrullination to be activated or deactivated, given the profound molecular effects of this modification. A prominent PAD substrate is fibrinogen, which promotes angiogenesis [46], and to date, no other significant proteins from an angiogenic perspective were shown to be affected by citrullination.

Recently, PAD4 has been shown to be an important component in the activation of the PI3K/AKT pathway [47, 48], which is an important regulator of VEGFA production [49]. In addition, PAD2 may be involved in the activation of Akt and downstream cancer progression, as BBCLA treatment of retinoblastoma cell line Y79 reduced the levels of activated Akt [50]. Our observation that all three PAD inhibitors reduce Akt Serine 473 phosphorylation by > 60% (Fig. 7A, 7B) suggests that inhibition of the PI3K/AKT signaling pathway is among downstream events secondary to PADs inhibition by BBCLA, CLA, and FA. Surprisingly, given the significant changes in activated Akt, no changes in total Akt and PI3K protein expression levels were noticeable, and the level of GSK3 β a protein downstream of the pathway, was reduced only upon FA treatment (Fig. 7A, 7B). Inhibition of Akt phosphorylation provides a molecular background for the observed anti-angiogenic effect, as the PI3K/Akt pathway is widely regarded as the key regulator of angiogenesis and Akt activation is one of the most important events in mitogenic cell signaling [51, 52, 53]. All three PAD inhibitors act in a similar manner in our ECs model, with lowered Akt phosphorylation, possibly dependent on the decreased levels of its activators, such as VEGFA and IL6, or through other mechanism(s) which should be addressed in further studies. The occurrence of angiogenesis depends on the activation of the three VEGF receptors (VEGFRs) tyrosine kinases by the hormones VEGF A, B, and C [54], which act intracellularly by activating, among others, the PI3K-Akt signaling pathway [55], which we showed to be affected by PAD inhibitors treatment. Whether other mitogenic signaling cascades, and particularly the RAS-Raf-MAPK signaling, are affected by PAD inhibitors in endothelial cells remains to be determined.

Our findings complement the limited existing studies regarding the role of PAD activity in angiogenesis and endothelial biology [56, 57]. We showed that irreversible PAD inhibitors affect key endothelial cell processes, such as capillary tube formation and wound healing, by lowering the capacity of cells to destabilize the ECM, inducing PEDF expression and secretion, decreasing VEGF expression and secretion, affecting the expression of cyclin CCNE and CCND, and, most importantly, lowering the levels of activated Akt. The results presented in this study provide further evidence that citrullination and PAD inhibitors may prove to be therapeutic targets, not only in autoinflammatory disorders but also in other pathologies. Based on the isoform-specific inhibitory potencies of the three inhibitors we used (Table 2) and the prominent effects of BBCLA, we infer that PAD4, which contains a nuclear localization signal (NLS) [58] and is strongly inhibited by BBCLA, may be the main isoform mediating endothelial histone citrullination. However, this hypothesis needs to be further validated using a specific knockout of each PAD isoform.

Conclusion

To summarize, we show that pharmacological inhibition of PADs in ECs resulted in subsequent significant decrease in histone citrullination, capillary-tube like formation, wound healing, Akt phosphorylation and expression/secretion of selected angiogenic factors. The obtained data indicate a possible role for citrullination in the regulation of angiogenesis.

Acknowledgements

Author Contributions

AB and OC conceived the study and its design; AB and OC developed the methods and performed experiments; All authors analyzed and interpreted the data and collectively wrote the manuscript.

Funding Sources

The presented study was supported by the Polish Ministry of Higher Education under Diamond Grant (2019-2023): DI2018 018948 and by the financing provided by The BioMedChem Doctoral School of University of Lodz and Polish Academy of Sciences.

Statement of Ethics

The study design and protocol involving the use of human umbilical cords were approved by the Bioethics Commission at the University of Lodz (Decision No. 15/KBBN-UŁ/III/2019 and 16 (III)/KBBN-UŁ/I/2021-22), all research was performed in accordance with relevant regulations and the guidelines of the Declaration of Helsinki. Informed consent was obtained from the donors at the Medeor Multidisciplinary Hospital in Lodz, no data regarding the donors were collected and stored, and the samples were completely anonymized.

Disclosure Statement

The authors have no conflicts of interest to declare.

References

- 1 Folkman J: Angiogenesis. *Annual Review of Medicine* 2006;57:1–18.
- 2 Chung AS, Ferrara N: Developmental and pathological angiogenesis. *Annual Review of Cell and Developmental Biology* 2011;27:563–584.
- 3 Cao Y, Arbiser J, D'Amato RJ, D'Amore PA, Ingber DE, Kerbel R, et al.: Forty-year journey of Angiogenesis Translational Research. *Science Translational Medicine* 2011;3.
- 4 Kerbel RS: Tumor angiogenesis. *New England Journal of Medicine* 2008;358:2039–2049.
- 5 Fadini GP, Albiero M, Bonora BM, Avogaro A: Angiogenic abnormalities in diabetes mellitus: Mechanistic and clinical aspects. *The Journal of Clinical Endocrinology & Metabolism* 2019;104:5431–5444.
- 6 Cheng R, Ma J: Angiogenesis in diabetes and obesity. *Reviews in Endocrine and Metabolic Disorders* 2015;16:67–75.
- 7 Pirola L, Balcerczyk A, Tothill RW, Haviv I, Kaspi A, Lunke S, et al.: Genome-wide analysis distinguishes hyperglycemia regulated epigenetic signatures of primary vascular cells. *Genome Research* 2011;21:1601–1615.
- 8 Miao F, Chen Z, Genuth S, Paterson A, Zhang L, Wu X, et al.: Evaluating the role of epigenetic histone modifications in the metabolic memory of type 1 diabetes. *Diabetes* 2014;63:1748–1762.
- 9 Yu K, Proost P: Insights into peptidylarginine deiminase expression and citrullination pathways. *Trends in Cell Biology* 2022;32:746–761.
- 10 Mondal S, Thompson PR: Chemical Biology of protein citrullination by the protein arginine deiminases. *Current Opinion in Chemical Biology* 2021;63:19–27.
- 11 Witalison E, Thompson P, Hofseth L: Protein arginine Deiminases and associated citrullination: Physiological functions and diseases associated with dysregulation. *Current Drug Targets* 2015;16:700–710.
- 12 Rebak AS, Hendriks IA, Elsborg JD, Buch-Larsen SC, Nielsen CH, Terslev L, et al.: A quantitative and site-specific atlas of the citrullinome reveals widespread existence of citrullination and insights into PAD14 substrates. *Nat Struct Mol Biol.* 2024 Feb 6. doi: 10.1038/s41594-024-01214-9.
- 13 Wang L, Song G, Zhang X, Feng T, Pan J, Chen W, et al.: PAD12-mediated Citrullination promotes prostate cancer progression. *Cancer Research* 2017;77:5755–5768.
- 14 Neeli I, Khan SN, Radic M: Histone deimination as a response to inflammatory stimuli in neutrophils. *The Journal of Immunology* 2008;180:1895–1902.
- 15 Ciesielski O, Biesiekierska M, Panthu B, Soszyński M, Pirola L, Balcerczyk A: Citrullination in the pathology of inflammatory and autoimmune disorders: Recent advances and future perspectives. *Cellular and Molecular Life Sciences* 2022;79.
- 16 Brinkmann V, Reichard U, Goosmann C, Fauler B, Uhlemann Y, Weiss DS, et al.: Neutrophil extracellular traps kill bacteria. *Science* 2004;303:1532–1535.
- 17 Mutua V, Gershwin LJ: A review of neutrophil extracellular traps (nets) in disease: Potential anti-nets therapeutics. *Clinical Reviews in Allergy & Immunology* 2020;61:194–211.
- 18 Manda-Handzlik A, Bystrzycka W, Cieloch A, Glodkowska-Mrowka E, Jankowska-Steifer E, Heropolitanska-Pliszka E, et al.: Nitric oxide and peroxynitrite trigger and enhance release of neutrophil extracellular traps. *Cellular and Molecular Life Sciences* 2019;77:3059–3075.
- 19 Fuchs TA, Brill A, Duerschmied D, Schatzberg D, Monestier M, Myers DD, et al.: Extracellular DNA traps promote thrombosis. *Proceedings of the National Academy of Sciences* 2010;107:15880–15885.
- 20 Martinod K, Demers M, Fuchs TA, Wong SL, Brill A, Gallant M, et al.: Neutrophil histone modification by peptidylarginine deiminase 4 is critical for deep vein thrombosis in mice. *Proceedings of the National Academy of Sciences* 2013;110:8674–8679.
- 21 Meegan JE, Yang X, Beard RS, Jannaway M, Chatterjee V, Taylor-Clark TE, et al.: Citrullinated histone 3 causes endothelial barrier dysfunction. *Biochemical and Biophysical Research Communications* 2018;503:1498–1502.
- 22 Osca-Verdegal R, Beltrán-García J, Paes AB, Nacher-Sendra E, Novella S, Hermenegildo C, et al.: Histone citrullination mediates a protective role in endothelium and modulates inflammation. *Cells* 2022;11:4070.
- 23 Jaffe EA, Nachman RL, Becker CG, Minick CR: Culture of human endothelial cells derived from umbilical veins. Identification by morphologic and immunologic criteria. *Journal of Clinical Investigation* 1973;52:2745–2756.

- 24 Ciesielski O, Biesiekierska M, Balcerczyk A: Epigallocatechin-3-gallate (EGCG) alters histone acetylation and methylation and impacts chromatin architecture profile in human endothelial cells. *Molecules* 2020;25:2326.
- 25 Wojtala, Dąbek, Rybaczek, Śliwińska, Świdorska, Słapek, et al.: Silencing lysine-specific histone demethylase 1 (LSD1) causes increased HP1-positive chromatin, stimulation of DNA repair processes, and dysregulation of proliferation by Chk1 phosphorylation in human endothelial cells. *Cells* 2019;8:1212.
- 26 Livak KJ, Schmittgen TD: Analysis of relative gene expression data using real-time quantitative PCR and the 2- $\Delta\Delta$ CT method. *Methods* 2001;25:402–408.
- 27 Wojtala M, Rybaczek D, Wielgus E, Sobalska-Kwapis M, Strapagiel D, Balcerczyk A. The role of lysine-specific demethylase 1 (LSD1) in shaping the endothelial inflammatory response. *Cellular Physiology and Biochemistry* 2021;55.
- 28 Carpentier, G. Protein array analyzer for ImageJ. Faculté des Sciences et Technologie, Université Paris Est Creteil, Val de Marne, France Available at <http://image.bio.methods.free.fr/ImageJ/Protein-Array-Analyzer-for-ImageJ.html> Accessed January 8, 2023.
- 29 Carpentier G, Berndt S, Ferratge S, Rasband W, Cuendet M, Uzan G, et al.: Angiogenesis analyzer for imagej — a comparative morphometric analysis of “Endothelial Tube Formation Assay” and “Fibrin bead assay.” *Scientific Reports* 2020;10:11568.
- 30 Suarez-Arnedo A, Torres Figueroa F, Clavijo C, Arbeláez P, Cruz JC, Muñoz-Camargo C: An image J plugin for the high throughput image analysis of *in vitro* scratch wound healing assays. *PLOS ONE* 2020;15.
- 31 Xu S, Alam S, Margariti A: Epigenetics in vascular disease – therapeutic potential of New Agents. *Current Vascular Pharmacology* 2014;12:77–86.
- 32 Balcerczyk A, Rybaczek D, Wojtala M, Pirola L, Okabe J, El-Osta A: Pharmacological inhibition of arginine and lysine methyltransferases induces nuclear abnormalities and suppresses angiogenesis in human endothelial cells. *Biochemical Pharmacology* 2016;121:18–32.
- 33 Wojtala M, Macierzyńska-Piotrowska E, Rybaczek D, Pirola L, Balcerczyk A: Pharmacological and transcriptional inhibition of the G9A histone methyltransferase suppresses proliferation and modulates redox homeostasis in human microvascular endothelial cells. *Pharmacological Research* 2018;128:252–263.
- 34 Chen H, Wei L, Luo M, Wang X, Zhan Y, Mao Y, et al.: PAD4 Inhibitor Promotes DNA damage and Radiosensitivity of Nasopharyngeal Carcinoma Cells. *Environmental Toxicology* 2021;36:2291–2301.
- 35 Ghajar CM, George SC, Putnam A: Matrix metalloproteinase control of capillary morphogenesis. *Critical Reviews™ in Eukaryotic Gene Expression* 2008;18:251–278.
- 36 Rohani MG, Parks WC: Matrix Remodeling by MMPs During Wound Repair. *Matrix Biology* 2015;44–46:113–121.
- 37 Thompson PR: Citrullination inhibits serpin activity. *The FASEB Journal* 2018;32:104.3.
- 38 Tilwawala R, Nemmara VV, Reyes AC, Sorvillo N, Salinger AJ, Cherpokova D, et al.: The role of Serpin citrullination in thrombosis. *Cell Chemical Biology* 2021;28:1728-1739.
- 39 Stefansson S, Petitclerc E, Wong Michael KK, McMahon GA, Brooks PC, Lawrence DA: Inhibition of angiogenesis *in vivo* by plasminogen activator inhibitor-1. *Journal of Biological Chemistry* 2001;276:8135–8141.
- 40 Stepanova V, Jayaraman P-S, Zaitsev SV, Lebedeva T, Bdeir K, Kershaw R, et al.: Urokinase-type plasminogen activator (UPA) promotes angiogenesis by attenuating proline-rich homeodomain protein (PRH) transcription factor activity and de-repressing vascular endothelial growth factor (VEGF) receptor expression. *Journal of Biological Chemistry* 2016;291:15029–15045.
- 41 Michalczyk ER, Chen L, Fine D, Zhao Y, Mascarinas E, Grippo PJ, et al.: Pigment epithelium-derived factor (PEDF) as a regulator of wound angiogenesis. *Scientific Reports* 2018;8:11142.
- 42 Belkacemi L, Zhang SX: Anti-tumor effects of pigment epithelium-derived factor (PEDF): Implication for cancer therapy. A mini-review. *Journal of Experimental & Clinical Cancer Research* 2016;35:10.1186/s13046-015-0278-7.
- 43 Martin D, Galisteo R, Gutkind JS: CXCL8/IL8 stimulates vascular endothelial growth factor (VEGF) expression and the autocrine activation of VEGFR2 in endothelial cells by activating NFκB through the CBM (CARMA3/BCL10/malt1) complex. *Journal of Biological Chemistry* 2009;284:6038–6042.
- 44 Sharma P, Azebi S, England P, Christensen T, Møller-Larsen A, Petersen T, et al.: Citrullination of histone H3 interferes with HP1-mediated transcriptional repression. *PLoS Genetics* 2012;8:e1002934.

Ciesielski et al.: Peptidylarginine Deiminases Inhibitors Attenuate the Endothelial Cells Angiogenic Potential

- 45 Dave JM, Bayless KJ: Vimentin as an integral regulator of cell adhesion and endothelial sprouting. *Microcirculation* 2014;21:333–344.
- 46 Shiose S, Hata Y, Noda Y, Sassa Y, Takeda A, Yoshikawa H, et al.: Fibrinogen stimulates *in vitro* angiogenesis by choroidal endothelial cells via autocrine VEGF. *Graefes' Archive for Clinical and Experimental Ophthalmology* 2004;242:777–783.
- 47 Chen H, Wei L, Luo M, Wang X, Zhu C, Huang H, et al.: Linc00324 suppresses apoptosis and autophagy in nasopharyngeal carcinoma through upregulation of PAD4 and activation of the PI3K/akt signaling pathway. *Cell Biology and Toxicology* 2021;38:995–1011.
- 48 Shen S, Wang X, Lv H, Shi Y, Xiao L: PADI4 mediates autophagy and participates in the role of Ganoderic acid monomers in delaying the senescence of alzheimer's cells through the AKT/mtor pathway. *Bioscience, Biotechnology, and Biochemistry* 2021;85:1818–1829.
- 49 Jiang B-H, Liu L-Z: PI3K/PTEEN signaling in tumorigenesis and Angiogenesis. *Biochimica et Biophysica Acta (BBA) - Proteins and Proteomics* 2008;1784:150–158.
- 50 Kim S, Song Y, Cho C, Kim H, Fang S, Jo D, et al.: Inhibition of protein arginine deiminase II suppresses retinoblastoma in orthotopic transplantation in mice. *Oncology Reports* 2023;50:146.
- 51 Somanath PR, Razorenova OV, Chen J, Byzova TV: Akt1 in endothelial cell and angiogenesis. *Cell Cycle* 2006;5:512–518.
- 52 Lee MY, Luciano AK, Ackah E, Rodriguez-Vita J, Bancroft TA, Eichmann A, et al.: Endothelial AKT1 mediates angiogenesis by phosphorylating multiple angiogenic substrates. *Proceedings of the National Academy of Sciences* 2014;111:12865–12870.
- 53 Shiojima I, Walsh K: Role of Akt signaling in vascular homeostasis and angiogenesis. *Circulation Research* 2002;90:1243–1250.
- 54 Claesson-Welsh L: Signal transduction by vascular endothelial growth factor receptors. *Vascular Pharmacology* 2012;56:308.
- 55 Jiang B-H, Liu L-Z: PI3K/PTEEN signaling in tumorigenesis and Angiogenesis. *Biochimica et Biophysica Acta (BBA) - Proteins and Proteomics* 2008;1784:150–158.
- 56 Khajavi M, Zhou Y, Birsner AE, Bazinet L, Rosa Di Sant A, Schiffer AJ, et al.: Identification of PADI2 as a novel angiogenesis-regulating gene by genome association studies in mice. *PLOS Genetics* 2017;13:e1006848.
- 57 Horibata S, Rogers KE, Sadegh D, Anguish LJ, McElwee JL, Shah P, et al.: Role of peptidylarginine deiminase 2 (PAD2) in mammary carcinoma cell migration. *BMC Cancer* 2017;17:378.
- 58 Wang Y, Chen R, Gan Y, Ying S: The roles of pad2- and pad4-mediated protein citrullination catalysis in cancers. *International Journal of Cancer* 2020;148:267–276.